

Pipelike current-carrying vortices in two-component condensates

M. N. Chernodub^{1,2,*} and A. S. Nedelin^{3,4}

¹*Laboratoire de Mathématiques et Physique Théorique, Université François-Rabelais Tours, Fédération Denis Poisson - CNRS, Parc de Grandmont, 37200 Tours, France*

²*Department of Physics and Astronomy, University of Gent, Krijgslaan 281, S9, B-9000 Gent, Belgium*

³*Department of Physics and Astronomy, Uppsala University, P.O. Box 803, Uppsala, S-75108, Sweden*

⁴*Institute for Theoretical and Experimental Physics, B. Chermushkinskaya 25, Moscow, 117218, Russia*

(Dated: August 30, 2018)

We study straight vortices with global longitudinal currents in the Bogomolny limit of the Abelian Higgs model with two charged scalar fields. The model possesses global $SU(2)$ and local electromagnetic $U(1)$ symmetries spontaneously broken to global $U(1)$ group, and corresponds to a semilocal limit of the standard electroweak model. We show that the contribution of the global $SU(2)$ current to the vortex energy is proportional to the total current squared. Locally, these vortices carry also longitudinal electromagnetic currents, while the total electromagnetic current flowing through a transverse section of the vortex is always zero. The vortices with high winding numbers have, in general, a nested pipelike structure. The magnetic field of the vortex is concentrated at a certain distance from the geometric center of the vortex, thus resembling a “pipe.” This magnetic pipe is layered between two electrically charged pipes that carry longitudinal electric currents in opposite directions.

PACS numbers: 03.75.Mn, 03.75.Lm, 12.15.-y

I. INTRODUCTION

Certain extended topological defects are able to support longitudinal currents. A well-known example of such a defect is the Abrikosov–Nielsen–Olesen vortex solution [1] in a $U(1) \times U(1)$ model [2]: the corresponding vortex string may carry both bosonic and fermionic superconducting flows of large magnitude. Loops of these superconducting strings may have various cosmological consequences [3].

The extended topological structures with longitudinal currents appear also at much smaller scales in the context of condensed matter physics. For example, vortices that carry longitudinal superfluid flow in a superfluid $^3\text{He-A}$ were proposed theoretically in Ref. [4]. Later, certain signatures of these stringy objects, known as w vortices, were found in nuclear magnetic resonance experiments [5] (see Ref. [6] for a detailed review).

The symmetry patterns and the zoo of the topological defects in the superfluid ^3He have a lot in common with the corresponding properties of the standard electroweak model in particle physics [7]. Thus it is not surprising that one of the most interesting realizations of the current-carrying strings in the field theory context appears in the standard model of electroweak interactions. This model supports various (embedded) topological defects including well-known Z - and W vortices [8, 9]. In a semilocal limit of the model (characterized by a special value of the Weinberg angle, $\theta_W = \pi/2$) these vortex solutions are known to carry persistent longitudinal currents of isocharge associated with the global symmetry

subgroup [10]. The word “semilocal” indicates that the symmetry group of the model is a product of the local electromagnetic group, $U_{e.m.}(1)$, and the global isosymmetry group, $SU_I(2)$. In this limit the original non-Abelian *gauge* group decouples from the scalar fields, and the resulting theory is basically the Abelian Higgs model with two complex scalar fields.

Beyond the semilocal limit (i.e., at any value of Weinberg’s angle) the current-carrying solutions were constructed in Refs. [11, 12] and evidence of their perturbative stability was found [12]. We refer an interested reader to the reviews [13] and [14] for an extended discussion of the vortex solutions in the standard electroweak model.

In the semilocal limit the vortices with nonzero longitudinal isocurrents exist only in type-II regime [10] because the energy per unit vortex length of such vortices diverges as the system approaches the boundary between type-II and type-I superconductivity. This boundary is known as the Bogomolny limit [15]. General vortex solutions without longitudinal currents were described in the Bogomolny limit of the semilocal model in Ref. [16]. The (iso)charged vortex solutions with persistent longitudinal currents were found in the same limit in Ref. [17]. We continue this line of investigation by studying in details the current-carrying vortex solutions in the Bogomolny limit of the Abelian with two Higgs fields. We concentrate on the current-carrying vortices with multiple winding numbers because these vortices – contrary to the elementary vortices with a unit winding number [17] – do have a finite energy per unit vortex length.

Our study is also motivated by the (theoretically anticipated and/or experimentally found) existence of various systems with multiple-component order parameters such as the already mentioned superfluid ^3He [6], two-

* On leave from ITEP, Moscow, Russia.

component Bose-Einstein condensates [18], two-band superconductors that includes the well-studied system of MgB₂ [19], liquid metallic hydrogen [20], two-component plasmas [21] etc.

The structure of this paper is as follows. In Sec. II we describe the Abelian model with two charged scalar complex fields. This model admits vortex solutions to the classical equation of motion, which are drastically simplified in the Bogomolny limit. Section III is devoted to the illustration of various multivortex solutions in this limit. We concentrate on the vortices with high winding numbers which have a “pipelike” structure: the magnetic field in such vortices is nonzero only in a thin region located at a certain fixed distance from the geometrical center of the vortex. In Sec. IV we introduce a longitudinal wave along the vortex and check that this wave corresponds to a current-carrying solution that satisfies the original (second-order) classical equations of motion. Finally, in Sec. V we calculate the energy per unit length of these vortices. The last section is devoted to our conclusion.

II. TWO-COMPONENT MODEL

The Lagrangian of the two-component Ginzburg-Landau model is

$$\mathcal{L} = -\frac{1}{4}F_{\mu\nu}F^{\mu\nu} + \frac{1}{2}|D_\mu\Phi|^2 - \lambda(|\Phi|^2 - \eta^2)^2, \quad (1)$$

where $F_{\mu\nu} = \partial_\mu A_\nu - \partial_\nu A_\mu$ is the field strength tensor of the $U_{e.m.}(1)$ gauge field A_μ and $D_\mu = \partial_\mu + ieA_\mu$ is the corresponding covariant derivative, and $|\Phi|^2 \equiv \rho^2 = \Phi^\dagger\Phi$. The scalar field Φ has two complex-valued components,

$$\Phi = \begin{pmatrix} \rho_1 e^{i\varphi_1} \\ \rho_2 e^{i\varphi_2} \end{pmatrix} \equiv \rho \begin{pmatrix} e^{i\varphi_1} \cos\theta \\ e^{i\varphi_2} \sin\theta \end{pmatrix}, \quad (2)$$

where we introduced the parametrization in terms of the two phases $\varphi_{1,2} \in [-\pi, \pi)$, two condensates $\rho_{1,2}$ with

$$\rho = \sqrt{\rho_1^2 + \rho_2^2}, \quad (3)$$

and/or the angular variable $\theta \in [0, \pi)$.

The model (1) possess the symmetry

$$G = SU_I(2) \times U_{e.m.}(1), \quad (4)$$

where $SU_I(2)$ group rotates the Higgs fields in the isotopic space,

$$SU_I(2) : \begin{cases} \Phi \rightarrow U\Phi, \\ A_\mu \rightarrow A_\mu, \end{cases} \quad (5)$$

with $U \in SU_I(2)$, and the Abelian $U_{e.m.}(1)$ group corresponds to the local electromagnetic symmetry which affects the phases of the scalar field (2),

$$U_{e.m.}(1) : \begin{cases} \Phi \rightarrow e^{i\gamma(x)}\Phi, \\ A_\mu \rightarrow A_\mu - \frac{1}{e}\partial_\mu\gamma(x). \end{cases} \quad (6)$$

According to Eq. (6) both components of the scalar field (2) carry the same electric charge e .

The dimensionality of the symmetry group (4) indicates that there are four conserved Noether currents. The electric (super)current corresponds to the rotations in the $U_{e.m.}(1)$ direction,

$$J_\mu \equiv \rho^2 j_\mu = \frac{1}{2i}[\Phi^\dagger D_\mu\Phi - c.c.]. \quad (7)$$

For the sake of further convenience we introduced here the reduced electric current:

$$j_\mu = J_\mu/\rho^2. \quad (8)$$

The three other Noether currents can be grouped into the isovector field

$$\vec{K}_\mu = 2eJ_\mu\vec{n} - \rho^2\vec{n} \times \partial_\mu\vec{n}, \quad (9)$$

$$\vec{n} = \frac{\Phi^\dagger\vec{\tau}\Phi}{\Phi^\dagger\Phi}, \quad \vec{n}^2 = 1. \quad (10)$$

The isocurrent \vec{K}_μ corresponds to the isospinor rotations $SU_I(2)$. The unit isovector \vec{n} – that is constructed with the Pauli matrices $\vec{\tau} = (\tau^1, \tau^2, \tau^3)$ – transforms in adjoint representation of the $SU_I(2)$ subgroup (5). The Abelian gauge transformations (6) leave both the isocurrent (9) and the vector (10) intact.

It is convenient to make the rescaling,

$$\Phi \rightarrow \eta\Phi, \quad A_\mu \rightarrow \eta A_\mu, \quad x_\mu \rightarrow \frac{x_\mu}{e\eta}, \quad (11)$$

so that all variables appear to be dimensionless. Then the classical equations of motion of the model (1) are

$$\partial^\mu j_{\mu\nu} + \rho^2 j_\nu - \frac{1}{2}\partial^\mu f_{\mu\nu} = 0, \quad (12)$$

$$-\partial^2\rho + \frac{1}{4}\rho\partial_\mu\vec{n}\partial^\mu\vec{n} + \rho j_\mu j^\mu - 4\alpha\rho(\rho^2 - 1) = 0, \quad (13)$$

where we denoted $\alpha = \lambda/e^2$, and

$$j_{\mu\nu} = \partial_\mu j_\nu - \partial_\nu j_\mu, \quad (14)$$

$$f_{\mu\nu} = \vec{n} \cdot \partial_\mu\vec{n} \times \partial_\nu\vec{n}, \quad (15)$$

are the strength tensors for the (reduced) electric current j_μ , Eq. (8), and for the vector field \vec{n} , Eq. (10), respectively. Instead of the gauge-variant field A_μ we use below the gauge-invariant electric current j_μ as an independent variable. The change from gauge-variant variables A_μ and Φ to the gauge-invariant fields j_μ , \vec{n} and ρ , is commonly used in this model [22, 23].

Equations (12) and (13) are supplemented by the conservation laws of the electric current (7) and the isocurrent (9), respectively:

$$\partial_\mu J_\mu = 0, \quad \partial_\mu \vec{K}_\mu = 0. \quad (16)$$

III. PIPELIKE VORTEX SOLUTIONS IN BOGOMOLNY LIMIT

In this section we discuss known static straight vortexlike solutions to the classical equations of motion (12) and (13). These vortices do not carry longitudinal currents so that the corresponding solutions depend only on two-dimensional coordinates x_1 and x_2 . Since all vectors/tensors involving (at least one of) the components $\mu = 0, 3$ are zero, the system becomes effectively two-dimensional.

In a special limit,

$$\alpha \equiv \frac{\lambda}{e^2} = \frac{1}{8}, \quad (17)$$

the classical equations of motion (12) and (13) reduce to a simpler system of differential equations:

$$\partial_i \vec{n} + \epsilon_{ij} [\vec{n} \times \partial_j \vec{n}] = 0, \quad (18)$$

$$\frac{1}{x} \frac{\partial}{\partial x} \left[x \frac{\partial}{\partial x} (\log \rho) \right] + \frac{1}{2} (\rho^2 - 1) - \frac{f_{12}}{2} = 0, \quad (19)$$

where $x = |\vec{x}|$. The expressions for the electric current (7) and the isocurrent (9) are simplified as well:

$$J_i = -\epsilon_{ij} \rho \partial_j \rho, \quad \vec{K}_i = -\epsilon_{ij} \partial_j (\rho^2 \vec{n}). \quad (20)$$

The special choice of couplings (17) is known as the Bogomolny limit [15]. The vortex solutions of the ‘‘semilocal’’ Abelian two-Higgs model – that were first found in Ref. [8] – were subsequently studied in this limit in Refs. [9, 16]. A general solution to the classical equations of motion in the Bogomolny limit (17) has a nonzero condensate (3) at its origin and in general is dubbed as ‘‘skyrmion’’ (for a detailed review see Ref. [13]).

In the Bogomolny limit the magnetic flux of the vortex is quantized:

$$\mathcal{F} \equiv \oint_{C_\infty} dx_i A_i = \int d^2x B = \frac{2\pi}{e} k, \quad k \in \mathbb{Z}, \quad (21)$$

where

$$B = F_{12} \equiv j_{12} - \frac{1}{2e} f_{12} = \frac{e}{2} (1 - \rho^2), \quad (22)$$

is the magnetic field of the vortex. The first integration in Eq. (21) is taken over the spatial contour C_∞ with an infinitely large radius. The last relation in Eq. (22) is supported by equations of motion (19) and Eq. (20).

The string tension (i.e., the vortex energy per its unit length) is quantized as well (we restore η for a moment):

$$\begin{aligned} \sigma &= \int d^2x \left[\frac{1}{2} B^2 + |D_i \Phi|^2 + \lambda (|\Phi|^2 - \eta^2)^2 \right] \\ &= \frac{e\eta^2}{2} |\mathcal{F}| \equiv \pi\eta^2 |k|, \end{aligned} \quad (23)$$

where $i = 1, 2$ are two-dimensional indices in the transverse (with respect to the straight vortex) plane.

The validity of the quantization (21) can be checked in the angular parametrization of the scalar field (2). The energy functional (23) contains the scalar derivative squared,

$$\begin{aligned} |D_i \Phi|^2 &= (\partial_\mu \rho)^2 + \rho^2 (\partial_i \theta)^2 + J_i^2 \\ &+ \frac{\rho^2}{4} \sin^2 2\theta [\partial_\mu (\varphi_2 - \varphi_1)]^2, \end{aligned} \quad (24)$$

For the energy to be finite, a vacuum state is to be realized at the spatial infinity. This means that all four terms in Eq. (24) should be zero: the variables θ and $\rho \neq 0$ should be independent of the coordinates, and the electric current,

$$J_i = \rho (eA_i + \cos^2 \theta \partial_i \varphi_1 + \sin^2 \theta \partial_i \varphi_2), \quad (25)$$

should be vanishing at spatial infinity. Moreover, if at spatial infinity the angle θ does not take the specific values, $\theta_\infty \neq 0$ and $\theta_\infty \neq \pi/2$, then the two phases of the Higgs fields should be equal, $\varphi_1 = \varphi_2$. We then recover the quantization of the magnetic flux (21), where the number k gets interpreted as common winding number of the phases φ_1 and φ_2 . If either $\theta_\infty = 0$ or $\theta_\infty = \pi/2$, then $\varphi_1 \neq \varphi_2$ and at large distances the winding number is carried either by φ_1 or by φ_2 , respectively.

Using a stereographic projection one can parametrize the vector \vec{n} , Eq. (10), by a complex function $u = u(z)$ with $z = x_1 + ix_2$:

$$n_1 + in_2 = \frac{2u}{1 + |u|^2}, \quad n_3 = \frac{1 - |u|^2}{1 + |u|^2}. \quad (26)$$

Then the first equation of motion (18) is satisfied automatically provided u is a meromorphic function [16].

For a vortex located at the origin of the two-dimensional plane, the following boundary conditions are to be implied:

$$\lim_{z \rightarrow \infty} \vec{n} = (0, 0, 1)^T, \quad \lim_{z \rightarrow 0} \vec{n} = (0, 0, -1)^T, \quad (27)$$

where the first relation is the choice of the vacuum state. In terms of the function u the conditions (27) read as

$$u(z=0) = \infty, \quad u(z=\infty) = 0. \quad (28)$$

The suitable meromorphic function is

$$u = \left(\frac{a}{z} \right)^k, \quad (29)$$

where k is the mentioned winding number and

$$a = e\eta R_{\text{vort}} \quad (30)$$

is a dimensionless parameter which defines the size R_{vort} of the vortex core. This parameter is equivalent to the parameter ξ_0 of [9] and to the parameter $|q_0|$ of [16].

Substituting the solution (29) into Eq. (26) and, subsequently, into Eq. (15), one gets an expression for f_{12} . Then, introducing a normalized coordinate

$$\xi = \frac{x}{a} \equiv \frac{r}{R_{\text{vort}}}, \quad (31)$$

we rewrite the second equation of motion (19) as follows:

$$\frac{1}{\xi} \frac{\partial}{\partial \xi} \left[\xi \frac{\partial}{\partial \xi} (\log \rho) \right] + \frac{a^2}{2} (\rho^2 - 1) = \frac{2k^2 \xi^{2k-2}}{(\xi^{2k} + 1)^2}. \quad (32)$$

This equation fixes the behavior of the scalar condensate ρ as a function of distance from the vortex center ξ , Eq. (31); for fixed vorticity k , Eq. (21); and for the fixed size of the vortex core a , Eq. (30).

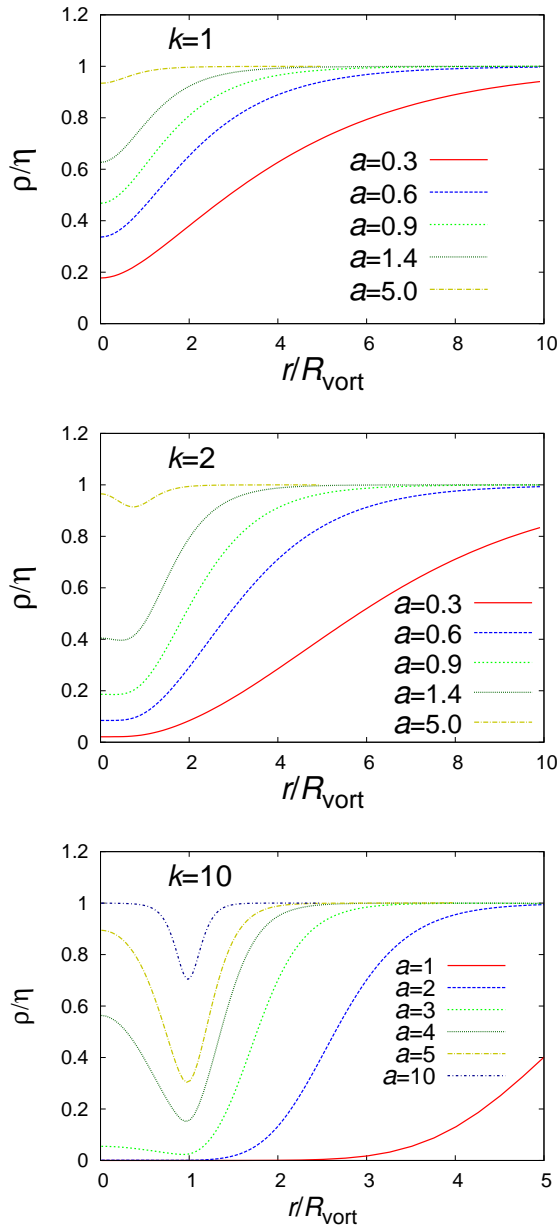


FIG. 1. Condensate ρ at the distance r from the vortex center for various sizes (thicknesses) of the vortex cores $R_{\text{vort}} = a/e\eta$. The vortices have vorticity numbers $k = 1$ (top), $k = 2$ (middle), and $k = 10$ (bottom).

The solutions of Eq. (32) can be found numerically. In Fig. 1 we show the condensate ρ , Eq. (3), for a vortex

carrying a single unit of the flux, $k = 1$ (the plot at the top); a double-flux vortex, $k = 2$ (the plot at the middle); and the high-vorticity solution, $k = 10$ (the plot at the bottom). One can observe that while the single-flux solutions $\rho = \rho(\xi)$ are always monotonic, the higher-flux solutions are not. A nonmonotonic density variation but for a different kind of vortices in a two-component model was also found in Ref. [26]. The solutions with a large-sized core ($a \gg 1$) and with a large flux ($k = 10$ in our example) have a well-recognized minimum around $r \approx R_{\text{vort}}$.

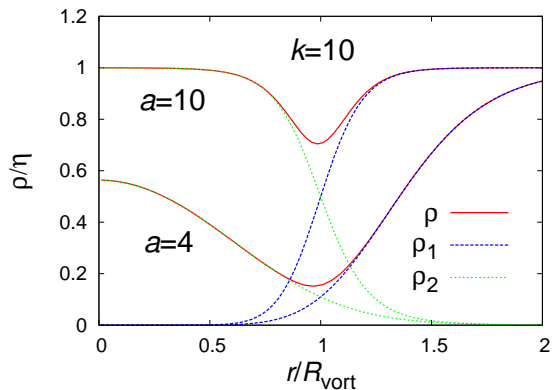


FIG. 2. Condensates ρ , ρ_1 and ρ_2 in high-vorticity ($k = 10$) solutions with two sizes $a = e\eta R_{\text{vort}}$ of the vortex cores.

The condensates for these vortex solutions are nonzero, $\rho \neq 0$, both at their centers, $r = 0$, and at spatial infinity, $\rho \rightarrow \infty$. As for the individual condensates, the ρ_1 condensate is vanishing at the center, while the ρ_2 condensate is zero at spatial infinity. This particular pattern of the condensates in the vortexlike solution is quite common for many-component systems. It appears in particle physics in the context of the standard electroweak model [13], and in the condensed matter physics: the corresponding structures were experimentally observed in a two-component condensate of ^87Rb atoms [18]. We plot the individual condensates of two solutions with $a = 4$ and $a = 10$ for the $k = 10$ vortex in Fig. 2.

In general, the magnetic field (22) of a vortex with a multiple vorticity is concentrated outside the center of the vortex. In Fig. 3 we show the density plots of the magnetic field in the transverse (x_1, x_2) plane for $k = 10$ vortices of different sizes R_{vort} . One can clearly see that the maximum of the magnetic field (darker regions) is distributed in a (generally) cylindrical thin region of the radius $R \simeq R_{\text{vort}} \equiv a/e\eta$. Thus, the magnetic field of the vortex is concentrated, basically, within a thin pipe of the radius R_{vort} . The magnetic field inside and outside the pipe is zero. A possible existence of similar solutions with pipelike (“helical”) structure in this model was discussed in [25]. The annular vortex solutions that somewhat resemble our pipelike solutions were also discussed in Refs. [23, 24].

The pipelike structure is well pronounced for large

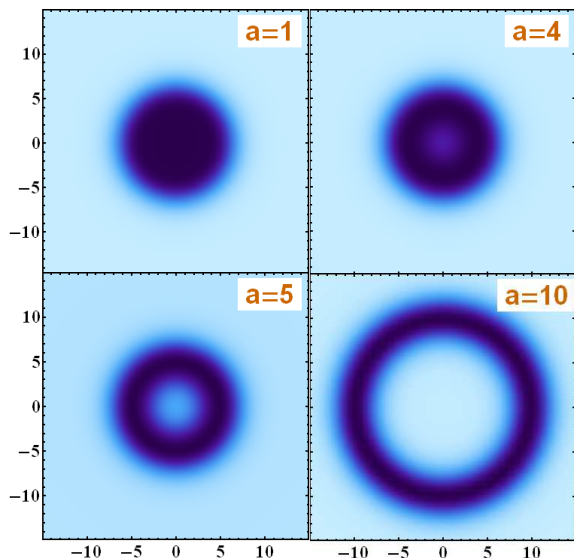


FIG. 3. Strength of the magnetic field (22) in high-vorticity ($k = 10$) solutions in the transverse plane. Various sizes of the vortex cores $R_{\text{vort}} = a/e\eta$ are shown. The spatial coordinates are given in units of $e\eta$.

($a \gg 1$) vortices with high-vorticity numbers. In a different context, vortices with high winding numbers were also studied in the standard electroweak model in [27].

Let us now consider the spatially-transverse component of the conserved isovector current (9) which corresponds to the flow of the global $SU_I(2)$ charge. The diagonal (in the isospace) component of this current is

$$K_i^{(3)}(\xi; k, a) = -\frac{\varepsilon_{ij} x_i}{a} \frac{\partial}{\partial \xi} \left[\frac{\xi^{2k} - 1}{\xi^{2k} + 1} \rho^2(\xi; k, a) \right]. \quad (33)$$

In the polar coordinates of the transverse plane, the radial component of the transverse isocurrent (33) is zero, $K_r^{(3)} = 0$. The angular component of this current is plotted in Fig. 4 for a few vortices with the large (fixed) winding number $k = 10$. The angular component exhibits a familiar pipelike structure with two peaks at moderate values of the vortex size a . These peaks are merged into one peak at larger values of a .

IV. LONGITUDINAL CURRENTS

The vortices may host certain waves that propagate freely along the vortices. The simplest way to introduce such a wave is to generalize the meromorphic function u [given, for a static solution, by Eq. (29)] as follows (remember that $z = x_1 + ix_2$):

$$u(x_1, x_2, x_3, x_4) = \left(\frac{a}{z}\right)^k e^{i(\omega x_0 - p_3 x_3)}. \quad (34)$$

Here the wave frequency $\omega \equiv p_0$ and the wave momentum p_3 are two unknown parameters. According to (11), in

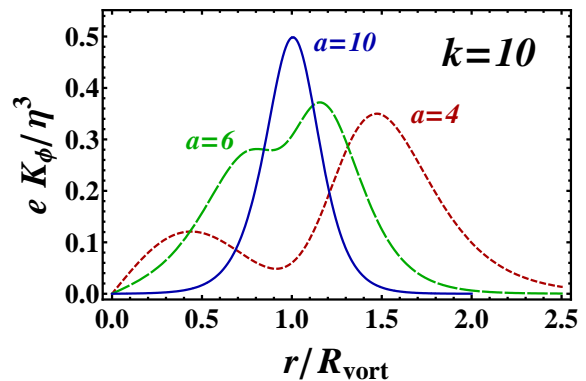


FIG. 4. The spatially transverse diagonal isocurrent (33) for vortices of various sizes a with a large winding number $k = 10$.

Eq. (34) the wave frequency ω and the wave momentum p_3 are given in units of $e\eta$.

According to Eq. (26) the ansatz (34) corresponds (up to a gauge transformation) to the following behavior of the scalar doublet (2):

$$\Phi = \begin{pmatrix} \rho_1(r) e^{ik\varphi} \\ \rho_2(r) e^{i(p_3 x_3 - \omega x_0)} \end{pmatrix}. \quad (35)$$

Here r and φ are the polar coordinates in the transverse plane and $\rho_{1,2}$ are certain functions of r . The form of Eq. (35) is essentially the same as in Refs. [10] and [17]. The ansatz (34) for the meromorphic function $u(z)$ was used in a different context in a $O(3)$ model in Ref. [28].

In analogy with the previous section, we substitute the ansatz (34) into the classical equations of motion, (12) and (13) using Eq. (26). The new equations also include the electric density, J_0 , and the longitudinal electric current J_3 , that are treated in these equations as the unknown independent functions. However, one can immediately figure out that the second-order differential equations (12) and (13) are self-consistent provided that

$$\omega = \pm p_3, \quad J_0(x) = \mp J_3(x) \equiv j\rho^2. \quad (36)$$

The first relation in Eq. (36) indicates that the longitudinal current is carried by massless waves. The second relation means that the regions with nonzero electric current density are always electrically charged. The signs in Eq. (36) distinguish between two possible directions of the wave propagation along the vortex.

The presence of the longitudinal currents does not influence the behavior of the condensate $\rho = \rho(r)$ because Eq. (32) is valid in the $J_0 \neq 0$ case. The transverse components, $\mu = 1, 2$, of the electric current J_μ are not modified by the presence of the longitudinal current as well, and Eq. (20) remains unaffected. As for the longitudinal components, the (reduced) electric charge density $j \equiv J_0/\rho^2$, Eq. (8) – or, equivalently, the longitudinal current density, Eq. (36) – is determined by the following differential relation:

$$\left[\frac{\partial^2}{\partial \xi^2} + \frac{1}{\xi} \frac{\partial}{\partial \xi} - a^2 \rho^2(\xi) \right] j(\xi) = \frac{4\omega k^2 \xi^{2k-2}}{(\xi^{2k} + 1)^3} (\xi^{2k} - 1). \quad (37)$$

A. Longitudinal electric current

The *total* longitudinal electric current $I_3^{\text{tot}} \equiv \int dx_1 dx_2 J_3$ streaming through any transverse plane of the vortex, and the total electric charge $\varrho^{\text{tot}} \equiv \int dx_1 dx_2 J_3$ per unit vortex length are both zero. Indeed, an integration of the left- and right-hand sides of Eq. (37) over the spatial coordinates of the two-dimensional transverse plane gives us the vanishing result:

$$\varrho^{\text{tot}} = \pm I_3 \equiv \int d^2r j(r) \rho^2(r) = 0. \quad (38)$$

Here we used the second equation in (36) and noticed that $\xi \frac{\partial}{\partial \xi} j(\xi) \rightarrow 0$ in the limits $\xi \rightarrow 0$ and $\xi \rightarrow \infty$.

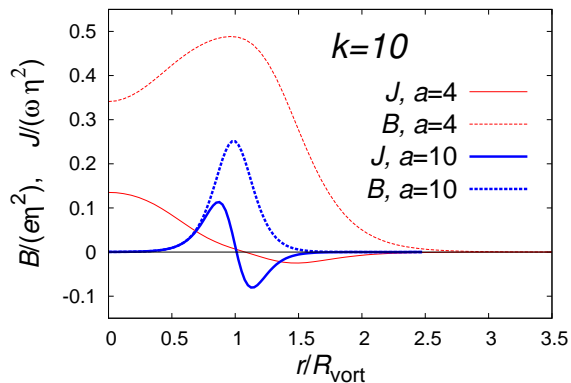


FIG. 5. Magnetic field B (the dashed lines) and the longitudinal electric current J (the solid lines) in the $k = 10$ vortex as the function of the radius r . The red/thin (blue/thick) lines correspond to the vortex of the size $a = 4$ ($a = 10$).

Despite the total electric current flowing through any transverse plane is zero, the local structure of the vortex in terms of electric currents is, however, nontrivial. In Fig. 5 we plot the density of the electric current and the strength of the magnetic field as functions of the distance to the vortex with the vorticity $k = 10$. We show these quantities for two vortices with the sizes $a = 4$ and $a = 10$. In both cases the electric current changes the sign at a certain nonzero distance R_0 from the center of the vortex,

$$J(R_0) = 0, \quad 0 < R_0 < \infty. \quad (39)$$

For a typical vortex the alternation of the current takes place at the value of the radius, that is approximately equal to the size of the vortex core, $R_0 \simeq R_{\text{vort}}$. As one can see from Fig. 5, it is the very radius where the magnetic field takes its maximum. The density of the current is positive in the inner core of the vortex, $r \lesssim R_{\text{vort}}$ and negative in the outer space, $r \gtrsim R_{\text{vort}}$.

In Fig. 6 we show a two-dimensional plot of the distribution of the *electric* current in the transverse plane of the $k = 10$ vortex of the size $a = 10$. The current is concentrated in the two nested narrow pipes that have

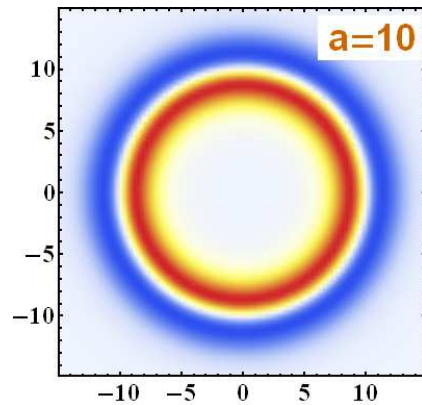


FIG. 6. The density of the longitudinal current – and, equivalently, the electric charge density – in the transverse plane of the $k = 10$ vortex of the size $a = 10$. The inner (red) pipe corresponds to the electric current flowing in the positive direction, while outer (blue) pipe denotes the density of the negatively directed current. There is almost no current inside the inner pipe and outside the outer pipe and also in between these two pipes.

relatively large diameters. The electric current is almost zero outside these pipes. Notice, that due to Eq. (36) the current-carrying pipes are also electrically charged. The electrically charged pipes enclose the pipe of the magnetic field, which was visualized in the lower right plot of Fig. 3. The interior and exterior of the vortex are oppositely charged, as illustrated in Fig. 6.

The distribution of the transverse electric currents in the transverse plane have a qualitative similarity with the distribution of the longitudinal currents, Fig. 3. The transverse currents – defined by the first relation in Eq. (20) – rotate in opposite directions inside and outside the pipe of the magnetic field. The transverse current density vanishes approximately at the radius of the magnetic pipe, similarly to the density of the longitudinal currents. These properties are the natural result of the nonmonotonic behavior of the condensate $\rho(r)$, Fig. 1. Physically, the outer current (say, circulating the vortex clockwise) generates the magnetic field along the z axis in an “outer” tube of a certain radius. The inner current (that rotates in the counterclockwise direction) leads to appearance of the magnetic field in the opposite direction in the “inner” tube. Since the inner and outer tubes have different radii, the resulting profile of the magnetic field has a maximum at a certain nonzero radius, thus forming a pipelike structure.

The total positive and negative longitudinal current, $I^{(\pm)} = \pm I^{\mp}$, can be calculated by integration over, say, the interior of the vortex core:

$$I \equiv |I^{(\pm)}| = \int_{r \leq R_0} d^2r J(r), \quad (40)$$

where we take, for definiteness, $J(r) > 0$. The radius R_0 is defined as a nonzero finite distance from the vortex center at which the electric current vanishes (39). The

integrated current (40) is shown in Fig. 7 as a function of the vortex size a for a few fixed vorticities. For small

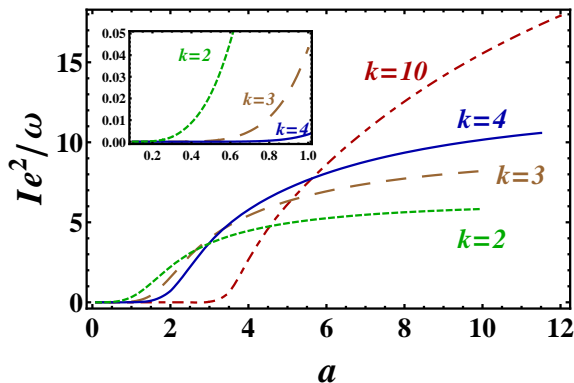


FIG. 7. The net positive/negative current (40) carried by interior/exterior of the vortex with the winding number k vs the vortex size $a = e\eta R_{\text{vort}}$. The inset shows zoom in on the region with $a < 1$.

vortices, $a \lesssim 1$, the total positive/negative current is very small. However, the inner and outer pipes of the thick vortices, $a \gtrsim 1$ may carry rather strong electric current. Moreover, the larger the transverse size of the vortex the stronger is the electric current [29].

Summarizing this section, we visualize the internal structure of the pipelike vortex in Fig. 8. The magnetic field has a pipelike profile shown by the green surface which is sandwiched in between two other pipes. The inner and outer pipes carry the electric currents in positive (shown by the red surface) and negative (the blue surface) directions, respectively. Since these electric currents in these pipes have both longitudinal and transverse components, the three-dimensional structure of the electric currents resembles spirals which are also visualized in Fig. 8.

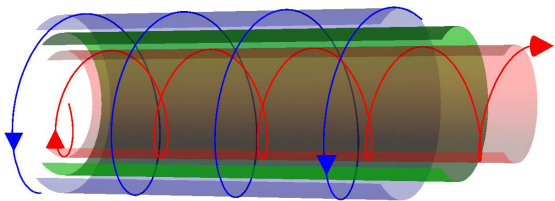


FIG. 8. A graphical representation of the structure of a thick ($a \gg 1$) vortex with a high winding number ($|k| \gg 1$). The pipelike magnetic field – shown by the green surface in the middle – is layered in between positive (inner) and negative (outer) electrically charged pipes (shown by the red and blue surfaces, respectively). These electric pipes carry helical electric currents in opposite directions. The arrows mark directions of the helical electric currents.

B. Longitudinal isocurrent

Now let us now consider the longitudinal components of the conserved isovector current (9). According to Eqs. (26) and (34), the off-diagonal components of the isocurrent, $K_\mu^{(1)}$ and $K_\mu^{(2)}$, are oscillating in time and space because they depend linearly on periodic functions $\cos \vartheta$ and $\sin \vartheta$, where $\vartheta = \omega(x_0 \pm x_3) - \varphi$. The diagonal components are time-independent quantities. The longitudinal isocurrent is

$$K_3^{(3)}(\xi; k, a) = -2\omega \frac{\rho^2(\xi; k, a)}{\xi^{2k} + 1} \left[\frac{\xi^{2k}}{\xi^{2k} + 1} + (1 - \xi^{2k})j(\xi; k, a) \Big|_{\omega=1} \right]. \quad (41)$$

The isocharge density, K_0 , is linked with the longitudinal isocurrent density, K_3 , in a manner of relation (36) for the electric charge/current density: $\vec{K}_3(x) = \pm \vec{K}_0(x)$. Both the isocharge density and the longitudinal isocurrent are proportional to the frequency parameter ω .

The longitudinal isocurrent (41) is shown in Fig. 9. This current has a two-peak structure for all studied values of the core size a . The peaks are centered near the values of the radius that approximately correspond to the extremes of the longitudinal electric current, plotted in Fig. 5 for $a = 4$ and $a = 10$.

In addition, Fig. 9 demonstrates that – unlike the ordinary electric current – the isocurrent density is either positively *or* negatively valued. Thus, the net isocurrent streaming along the vortex is nonvanishing and the vortex has a nonzero total isocharge. These global properties are qualitatively similar to the characteristics of the solutions with low winding numbers that were found in Refs. [10] and [17].

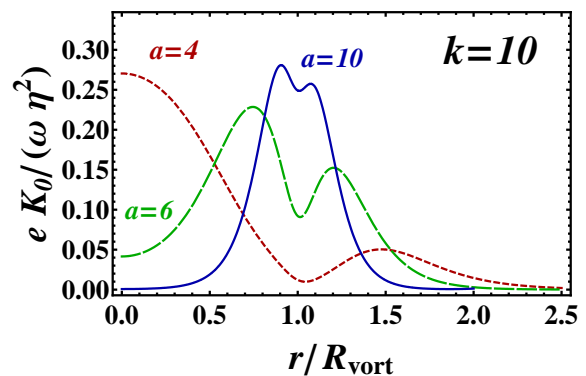


FIG. 9. The longitudinal isocurrent (41) for vortices of various sizes a with large winding number $k = 10$.

The absolute value of the total longitudinal isocurrent which is carried by the vortex,

$$K^{\text{tot}} = \left| \int d^2r K_3^{(3)}(r) \right|, \quad (42)$$

is shown in Fig. 10 as a function of the vortex core size a for a few values of the winding number k . The behav-

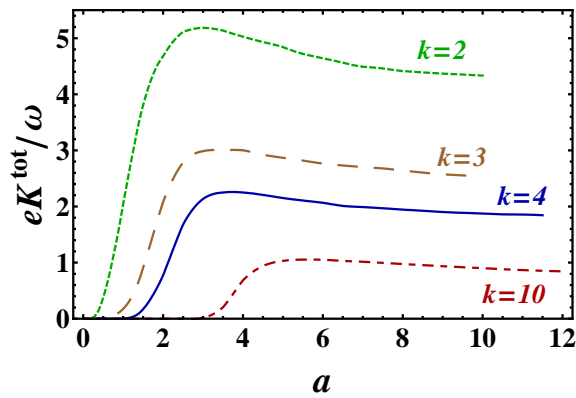


FIG. 10. The net longitudinal isocurrent (42) vs the vortex core size $a = e\eta R_{\text{vort}}$ for various winding numbers k .

ior of the new isocurrent (42) is similar to the net positive/negative electric current, Fig. 7. The total isocurrent is very small (at fixed ω) for small values of the vortex core size a . At a particular vortex size a , the isocurrent starts to grow quickly as a function of a . Then it reaches a maximum, and, unlike the positive/negative fraction of the electric current, the isocurrent slowly diminishes as the function of the vortex core size a . In general, the larger is the winding number k , the smaller is the net isocurrent.

Notice that the total longitudinal electric charge carried by the solutions vanishes exactly (38) because this current is generated by the *local* $U(1)$ symmetry (6). The net longitudinal isocurrent is not zero (42) since it carries the charges corresponding to the global $SU(2)$ subgroup of the model (5).

V. ENERGY OF VORTICES

A. Contribution of longitudinal current

In this section we calculate the energy of the vortices that is carried by the longitudinal currents in the Bogomolny limit. The energy momentum tensor of the Abelian two-Higgs model (1) is given by the following equation,

$$T_{\mu\nu} = -g_{\mu\nu}\mathcal{L} - F_{\mu}^{\sigma}F_{\nu\sigma} + \frac{1}{2}(D_{\mu}\Phi)^{\dagger}D_{\nu}\Phi + \frac{1}{2}(D_{\nu}\Phi)^{\dagger}D_{\mu}\Phi, \quad (43)$$

where $g_{\mu\nu}$ is the metric tensor. In the spherical isovector representation (10) the energy density reads as follows:

$$T_{00} = \frac{1}{2}(\partial_0\rho)^2 + \frac{1}{2}(\partial_i\rho)^2 + \frac{\rho^2}{8}(\partial_0\vec{n})^2 + \frac{\rho^2}{8}(\partial_i\vec{n})^2 + \lambda(\rho^2 - 1)^2 + \frac{\rho^2}{2}j_0^2 + \frac{\rho^2}{2}j_i^2 + \frac{1}{2}\left(j_{0i} - \frac{1}{2}f_{0i}\right)^2 + \frac{1}{4}\left(j_{ij} - \frac{1}{2}f_{ij}\right)^2. \quad (44)$$

We integrate Eq. (44) over the transverse coordinates x_1 and x_2 , imply the Bogomolny limit (17), and simplify the expression using both integration by parts and the corresponding equations of motion (18) and (18). As a result, we get the vortex energy per unit vortex length:

$$\sigma(k, a) \equiv \int d^2x T_{00} = \pi|k| + \chi(k, a)\omega^2. \quad (45)$$

The first term in the right-hand side of Eq. (45) corresponds to the energy of the vortex in the absence of the electric current (23). The second part is the contribution of the electric current to the vortex energy. This contribution is proportional to the wave frequency square, ω^2 or, equivalently, to the square of the total isocurrent carried by the vortex (42), or to the total electric current in, say, the inner charged pipe of the solution (40).

The dependence of the energy on the current is governed by the dimensionless coefficient χ that can be separated into three parts:

$$\chi(k, a) = \chi_1(k, a) + \chi_2(k, a) + \chi_3(k). \quad (46)$$

The first term in Eq. (46) is expressed via the condensate ρ ,

$$\chi_1(k, a) = 2\pi a^2 \int_0^{\infty} d\xi \frac{\xi^{2k+1}\rho^2(\xi; k, a)}{(\xi^{2k} + 1)^2}, \quad (47)$$

while the second term can be determined via the electric current density j

$$\chi_2(k, a) = 8\pi k^2 \int_0^{\infty} d\xi \frac{(\xi^{2k} - 1)\xi^{2k-1}}{(\xi^{2k} + 1)^3} j(\xi; k, a) \Big|_{\omega=1}, \quad (48)$$

The third term can be calculated exactly:

$$\chi_3(k) = 8\pi k^2 \int_0^{\infty} d\xi \frac{\xi^{4k-1}}{(\xi^{2k} + 1)^4} \equiv \frac{2\pi|k|}{3}. \quad (49)$$

The energy of the vortex (45) saturates the Bogomolny bound and it thus corresponds to the lowest possible energy for fixed parameters k , ω and a . Expressions (45)–(49) correspond to the lower bound on energy calculated previously in Ref. [10].

The first integral (47) diverges for $k = 1$. Indeed, at large transverse distances $\xi \gg 1$ the condensate is distance independent, $\rho \simeq 1$, and the integral in Eq. (47) becomes logarithmically divergent at large distances, $\int^{\xi_{\text{max}}} \xi^{-1} d\xi \sim \log \xi_{\text{max}}$. Thus, finite-sized vortices ($a \neq 0$) with a minimal winding number, $k = 1$, cannot carry the longitudinal currents in the Bogomolny limit. However, the vortices with higher vorticities, $k \geq 2$, can support the longitudinal currents in the this limit.

In the Bogomolny limit the energy of the currentless vortex – given by the first term in Eq. (45) – is independent of the vortex size a . Unexpectedly, in the presence

of a longitudinal current the energy becomes dependent on the vortex size parameter a . In Fig. 11 we plot χ as a function of the vortex size a for the same set of vorticities that was already selected for Fig. 7. Notice that despite

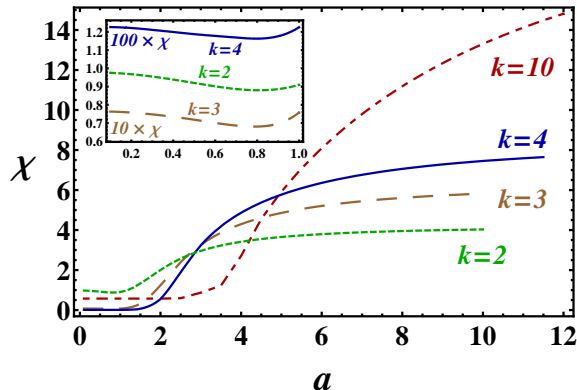


FIG. 11. The coefficient χ that determines the contribution of the electric current into the energy of the vortex (45). The inset shows a zoom in on a low- a region.

the fact that the curves in Fig. 7 and in Fig. 11 look similar on a qualitative level, they cannot be superimposed on each other by simple scale transformations.

According to Fig. 11, the excess of energy provided by the electric current is a monotonically increasing function of the vortex size at relatively large size a of the vortex core. A zoom in on the low- a region – shown in the inset of Fig. 11 – reveals a very shallow minimum at the fixed size of the vortex

$$a_{\min} \approx 0.8, \quad \text{or} \quad R_{\text{vort}} \approx \frac{0.8}{e\eta}, \quad (50)$$

for all studied vorticities $k \geq 2$.

Thus, in the Bogomolny limit a vortex with a fixed winding number $k > 1$ and a fixed frequency parameter $\omega \neq 0$ would tend to change its transverse size to the value (50) that corresponds to the global minimum of the vortex energy. According to the inset of Fig. 7, the electric current at $a \simeq a_{\min}$ is small but nonzero (we remind that the current can be made arbitrarily large by increasing the free parameter ω).

The vortex core tends to stabilize its transverse size at the value (50) for which the nested-pipe structure of the vortex interior cannot be resolved visually. This fact is seen in the behavior of the condensate ρ of the $a = 1$ vortex with the vorticity $k = 10$ (lowest panel of Fig. 1), or one can alternatively look at the magnetic field profile of the same vortex in Fig. 3. However, the minimum is very shallow so that a small perturbation – for example, induced by a shift of parameters towards type-II superconductivity – may shift the stability point to higher values of the vortex core radius a .

The dependence of the vortex energy per unit vortex length on the value of the electric current in one of the pipes I is shown in Fig. 12. At very low values of the current I the energy has a very shallow minimum which

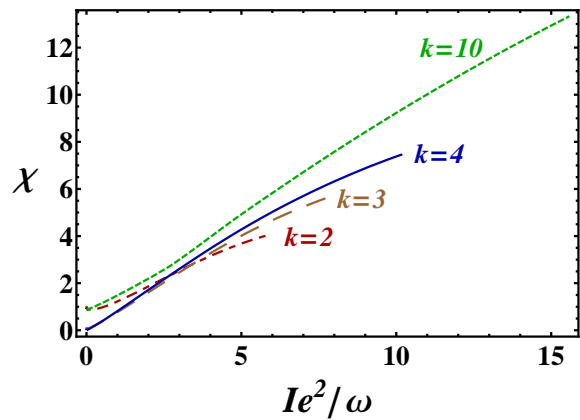


FIG. 12. The energy coefficient χ as a function of the (normalized) absolute value of the electric current flowing in, say, the inner charged pipe (40).

is visible in the plot of the $k = 2$ solution. At higher values of the current the energy is a monotonically rising function.

B. Rearrangement of vortex lattice

As we have already discussed, in the Bogomolny limit the energy per unit vortex length of an elementary ($k = 1$) vortex is infinite at any finite ω , or, equivalently, at any nonzero value of the longitudinal isocurrent. In the absence of the external isocurrent the total energy of a many-vortex configuration does not depend neither on positions of vortices nor on their sizes in this limit. Now, in a thought experiment, let us apply an external isocurrent K^{tot} along a configuration of an even number of parallel elementary vortices. Because of energy considerations it is clear that the elementary vortices would tend to merge together and form a set of, at least, double ($k = 2$) vortices that have a finite energy at the nonzero isocurrent. Then each of the $k = 2$ vortices would tend to adjust its transverse size a in such a way that the total energy is minimal at the fixed value of the isocurrent [30]. Thus, the presence of an external isocurrent should generally lead to rearrangement of the vortex ensembles.

A nonzero isocurrent (41) corresponds to a combination of two electric currents – carried by up and down components of the order parameter – for which the total electric current is zero. Although a realization of such an isocurrent in an experimental setup is an open issue, our result suggests that the vortex lattice should be restructured under the influence of the external isocurrent that is parallel to the external magnetic field. Also, our result shows that the multiple merging of the elementary vortices under the influence of the external isocurrent may lead to a formation of a vortex with a high winding number that exhibits the exotic “nested-pipe” structure.

We expect that our results are rather generic and they should not be limited strictly to the particular limit (17)

of the couplings. If the system is sufficiently close to the Bogomolny limit, then we expect that an external isocurrent would induce a rearrangement of the vortices in this system.

One of the well-studied examples of the two-band superconductor is MgB_2 [19]. In external magnetic field the vortex lattice in MgB_2 has quite specific geometrical patterns [31], that are imprinted by elementary vortices. Such an inhomogeneous distribution of vortices in multicomponent systems was first predicted theoretically in Ref. [32]. It would be interesting to check the effect of the external longitudinal isocurrent on the properties of the vortex lattice in this real material, which is rather far from the Bogomolny limit (17).

VI. CONCLUSION

We found pipelike vortex structures in an Abelian gauge model with two scalar condensates. This model possesses global $SU_I(2)$ symmetry (isosymmetry) as well as local $U_{e.m.}(1)$ symmetry corresponding to the Maxwell electromagnetism. The symmetry group is broken spontaneously to a global $U(1)$ subgroup. The model possesses vortices that are linelike topological defects which carry magnetic flux. We found that the vortices with high winding numbers and with large sizes of the vortex cores have the pipelike shape of the magnetic field: the magnetic field is concentrated at a certain distance from the geometric center of the vortex, thus resembling a pipe.

For the sake of simplicity we were working in the Bogomolny limit of the model in which the classical equations of motion are drastically simplified.

We show that nonelementary vortices in the Bogomolny limit of the model are able to support the longitudinal isocurrents that carry the isocharge along the vortices. The isocharge corresponds to the conserved Noether charge with respect to the diagonal component

of the global $SU_I(2)$ subgroup. The isocurrent is proportional to the difference between the electric currents carried by the upper and lower components of the order parameter. The current-carrying vortex also possesses a nonzero density of the isocharge localized in the vicinity of the vortex core. The elementary current-carrying vortices with unit vorticity have infinite energy per unit length, while the energies of the current-carrying vortices with multiple winding numbers are finite.

The total vortex energy is given by a sum of two terms. The first contribution is the standard Bogomolny term that is proportional to the magnetic flux inside the vortex. The second term comes due to the presence of the longitudinal current. This term is proportional to the total isocurrent squared. The dependence of the vortex energy on the isocharge current may lead to potentially observable effects like, for example, rearrangement of the positions of vortices in the vortex lattice of a two-band superconductor.

The vortices with large transverse sizes and with high winding numbers have a nested pipelike structure. In addition to the mentioned “magnetic pipe” that carries the magnetic flux of the vortex, the vortex also possesses two electrically charged pipes of larger and smaller radii. These “electric pipes” are oppositely charged and they also carry longitudinal electric currents of equal strength in opposite directions so that the net electromagnetic current flowing through a transverse section of the vortex is always zero. The magnetic pipe is always layered between the two electric pipes.

The authors are grateful to P. Forgacs, A. Niemi, M. Volkov and G. Volovik for interesting discussions, useful comments, and suggestions. This work has been supported by the French Agence Nationale de la Recherche project ANR-09-JCJC “HYPERMAG” and by the Swedish STINT Institutional Grant No. IG2004-2 025. M.N.Ch. is grateful to the members of the Department of Theoretical Physics at Uppsala University for the kind hospitality and stimulating environment.

-
- [1] A. A. Abrikosov, *Sov. Phys. JETP* **5**, 1174 (1957); H. B. Nielsen and P. Olesen, *Nucl. Phys.* **B61**, 45 (1973).
 - [2] E. Witten, *Nucl. Phys. B* **249**, 557 (1985).
 - [3] J. P. Ostriker, A. C. Thompson and E. Witten, *Phys. Lett. B* **180**, 231 (1986).
 - [4] G.E. Volovik, *JETP Lett.* **39**, 200 (1984).
 - [5] H.K. Seppälä, P.J. Hakonen, M. Krusius, T. Ohmi, M.M. Salomaa, J.T. Simola, and G.E. Volovik, *Phys. Rev. Lett.* **52**, 1802 (1984).
 - [6] M. M. Salomaa and G.V. Volovik, *Rev. Mod. Phys.* **59**, 533 (1987).
 - [7] G. E. Volovik, *Int. Ser. Monogr. Phys.* **117**, 1 (2006).
 - [8] T. Vachaspati and A. Achucarro, *Phys. Rev. D* **44**, 3067 (1991).
 - [9] M. Hindmarsh, *Phys. Rev. Lett.* **68**, 1263 (1992).
 - [10] P. Forgacs, S. Reuillon and M. S. Volkov, *Phys. Rev. Lett.* **96**, 041601 (2006) [arXiv:hep-th/0507246]; *Nucl. Phys. B* **751**, 390 (2006) [arXiv:hep-th/0602175].
 - [11] M. S. Volkov, *Phys. Lett. B* **644**, 203 (2007) [arXiv:hep-th/0609112].
 - [12] J. Garaud and M. S. Volkov, *Nucl. Phys. B* **826**, 174 (2010) [arXiv:0906.2996]; and arXiv:1005.3002.
 - [13] A. Achucarro and T. Vachaspati, *Phys. Rept.* **327**, 347 (2000) [arXiv:hep-ph/9904229].
 - [14] E. Radu and M. S. Volkov, *Phys. Rept.* **468**, 101 (2008) [arXiv:0804.1357].
 - [15] E. B. Bogomolny, *Sov. J. Nucl. Phys.* **24**, 449 (1976).
 - [16] G. W. Gibbons, M. E. Ortiz, F. Ruiz Ruiz and T. M. Samols, *Nucl. Phys. B* **385**, 127 (1992) [arXiv:hep-th/9203023].
 - [17] E. Abraham, *Nucl. Phys. B* **399**, 197 (1993).
 - [18] M.R. Matthews, B.P. Anderson, P.C. Haljan, D.S. Hall,

- C.E. Wieman, and E.A. Cornell, Phys. Rev. Lett. **83**, 2498 (1999).
- [19] J. Nagamatsu, N. Nakagawa, T. Muranaka, Y. Zenitani, and J. Akimitsu, Nature **410**, 63 (2001).
- [20] E. Babaev, A. Sudbo and N.W. Ashcroft, Nature **431**, 666 (2004).
- [21] L. D. Faddeev and A. J. Niemi, Phys. Rev. Lett. **85**, 3416 (2000) [arXiv:physics/0003083].
- [22] J. Govaerts, J. Phys. A **34**, 8955 (2001) [arXiv:hep-th/0007112]; E. Babaev, L. D. Faddeev and A. J. Niemi, Phys. Rev. B **65**, 100512(R) (2002) [arXiv:cond-mat/0106152].
- [23] J. Govaerts, D. Bertrand and G. Stenuit, Supercond. Sci. Technol. **14**, 463 (2001) [arXiv:cond-mat/0006070].
- [24] J. Govaerts, G. Stenuit, D. Bertrand, O. van der Aa, Phys.Lett. **A267**, 56 (2000) [arXiv:cond-mat/9908451].
- [25] A. J. Niemi, K. Palo and S. Virtanen, Phys. Rev. D **61**, 085020 (2000).
- [26] E. Babaev, J. Jäykkä, and M. Speight, Phys. Rev. Lett. **103**, 237002 (2009).
- [27] A. Achucarro, R. Gregory, J. A. Harvey and K. Kuijken, Phys. Rev. Lett. **72**, 3646 (1994) [arXiv:hep-th/9312034].
- [28] L. A. Ferreira, JHEP **0905**, 001 (2009) [arXiv:0809.4303].
- [29] Here we fix the value of the frequency parameter ω because of the proportionality law $I \propto \omega$ for the total current (40). We also remind a reader that the electric currents in inner and outer pipes flow in opposite directions. The total electric current streaming along the vortex is always zero, Eq. (38).
- [30] The variation of the vortex size at a fixed value of the isocurrent $K^{\text{tot}}(a, \omega) = \omega K^{\text{tot}}(a, \omega = 1)$ is realizable because of the presence of the free parameter ω . The parameter ω is to be adjusted properly to compensate variation in the current, Fig. 10, caused by the variation in the vortex size a .
- [31] V. Moshchalkov, M. Menghini, T. Nishio, Q. H. Chen, A. V. Silhanek, V. H. Dao, L. F. Chibotaru, N. D. Zhigadlo, J. Karpinski, Phys. Rev. Lett. **102**, 117001 (2009).
- [32] E. Babaev and M. Speight, Phys. Rev. B **72**, 180502(R) (2005).